

## Cell melodies: when sound speaks to stem cells

C. Ventura<sup>1,2,3</sup>, D. Gullà<sup>2</sup>, M. Graves<sup>2</sup>, A. Bergonzoni<sup>2</sup>, R. Tassinari<sup>3</sup>, C. Cavallini<sup>3</sup>, and J. von Stietenron<sup>2</sup>

<sup>1</sup>Istituto Nazionale di Biostrutture e Biosistemi (INBB), Laboratory of Molecular and Cellular Biology, University of Bologna, Bologna, Italy

<sup>2</sup>VID art|science/INBB, Bologna, Italy

<sup>3</sup>Stem Wave Institute for Tissue Healing (SWITH), Ettore Sansavini Health Science Foundation, Lugo (Ravenna), Italy

*Corresponding Author:* Carlo Ventura, MD, Ph.D; e-mails: ventura.vid@gmail.com or carlo.ventura@unibo.it

**Keywords:** Human adipose derived stem cells, Sound vibration, Music, Multi spectral imaging. Cellular vibration.

### ABSTRACT

**Background:** Our cells produce acoustic vibrations that may inform us of their state of health or disease. Music and voice, through the diffusive power of sound, permeate our body. Stem cells reside in all body tissues, orchestrating tissue repair throughout life. Can the sound of music and words affect human stem cells? This fascinating question has been the conductive theme of “Cell Melodies”, a world premier live experiment organized November 7<sup>th</sup>-9<sup>th</sup>, 2016 in Bologna, Italy, by VID art|science, an international movement of Artists and Scientists ([www.vidartscience.org](http://www.vidartscience.org)), and cured by Carlo Ventura, Professor of Molecular Biology and stem cell scientist at the University of Bologna, with Julia von Stietenron, Art Director of VID art|science.

**Materials and Methods:** On the scene, together with Milford Graves, a famous Jazz drummer based in New York, and Alessandro Bergonzoni, a renowned theater actor, there were human adipose-derived stem cells on the stage of a microscope equipped with a multi-spectral imaging (MSI) system. MSI allows information collection and processing across the electromagnetic spectrum (light), and was used to detect the electromagnetic emission spectra produced by stem cells in response to the sound patterns generated by the Artists. MSI data were projected onto a screen and made visible to the Audience.

**Results:** Different MSI patterns were generated by stem cells in response to different sound spectra produced by the Musician, whose performance sinks roots in the ancestral rhythms

and sounds from Africa and Latin America, using the heartbeat as the beginning of every possible pace.

MSI also revealed that stem cell emission spectra remarkably changed during the Actor’s performance, varying upon sound emission patterning created by his dialog.

**Conclusions:** For the first time, we provided evidence that human stem cells are able to respond with different vibrational signatures to the sound generated by Artists in the form of music or voice dialog in live performances.

Future experiments are warranted to reveal whether the observed cellular responses may be associated with changes in gene/protein expression and signaling pathways, being of relevance for human stem cell homeostasis.

### INTRODUCTION

In today’s technological age the increasing use of wireless technologies, Internet and mobile phones has made us more and more embedded within a world of physical signaling and informational processing. We are also becoming progressively aware of the vibratory nature of the Universe: quantum-scale objects, for example, are described in terms of particles and waves in quantum mechanics, and the wave-particle duality is exploited in electron microscopy and neutron diffraction. Compelling evidence is now showing that our cells are able to communicate through near-infrared light emission<sup>1,2</sup>, and can generate both electromagnetic signals<sup>3-5</sup> and mechanical/acoustic vibrations<sup>6-9</sup>.

Even at the cellular and molecular level, Life is shaped through recurrent rhythms. By using an instrumentation designed *ad hoc* to pump elec-

tromagnetic waves with different frequencies to a growing microtubule within an artificial cell-like environment, and using scanning tunneling microscopy (STM), defined resonance modes were found to exist between the tubulin protein structure and the applied frequencies<sup>3</sup>. Moreover, STM has revealed that single microtubule “tunneling current images” are produced when different resonance frequencies are pumped simultaneously<sup>3</sup>. The observation that only certain electromagnetic field frequencies could elicit peculiar conformational changes suggests that mechanical changes could be remotely tuned in a precise structural (anatomical) mode by employing electromagnetic fields remotely. Consonant with the relevance of the generation and spreading of biological information through vibrational processes is the evidence for the emission of high-frequency electric fields with radiation characteristics from microtubule<sup>4</sup> and even the detection of multi-level memory-switching properties at the level of a single brain microtubule<sup>5</sup>.

DNA itself may be considered as an electrically charged vibrational entity. In the cell nucleus, this macromolecule is subjected to the continuous assembly into multifaceted loops and domains by transcription factors and molecular motors. These events impart nanomechanical oscillatory features that could be essential for the storage and processing (expression) of genetic information. Accordingly, DNA has been found to exhibit wide-ranging electromagnetic resonance frequencies from THz to KHz spectra<sup>10</sup>.

The finding that microtubular activity is associated with the remarkable generation of electric fields, spreading information across the cells, provides novel cues for understanding cell-to-cell communication. Several proteins exhibit helix-turn-helix domains and can be viewed as oscillatory entities, the helices being like springs, with the turns acting as connectors between oscillators. A single protein can be assumed to be a phase-resonant vibrating system. Near terahertz field microscopy has recently been able to capture and characterize vibrations of proteins, tiny motions critical to human life. This finding indicates that, like the strings on a violin or the pipes of an organ, the proteins in the human body vibrate in different patterns<sup>11</sup>. Cellular proteins not only diffuse through water, but they predominantly “walk” on the microtubules by the aid of “molecular motors”, like kinesins and dyneins<sup>9</sup>. Within this context, signaling molecules

could be viewed as oscillators walking on the cytoskeletal network, with the microtubules dissipating the major vibrational differences among these oscillators. This suggests that oscillations of these complexes could achieve a synchronous state, and that synchronization of the oscillatory pattern may represent an essential feature in biomolecular recognition. The structure of the cytoskeleton and the nucleoskeleton could convey characteristics of connectedness, hence rhythmic behavior and synchronization modes could ultimately be transmitted up to and recorded from the cell surface. To this end, multispectral imaging (MSI) is currently emerging as a major tool to afford automated unbiased, non-invasive monitoring of cellular vibration patterning<sup>12-14</sup>. MSI provides a measurement of the electromagnetic radiation reflected from an object or scene (i.e., materials in the image) at many narrow wavelength bands. By the aid of a multispectral camera adapted to the stage of an inverted microscope, it is now possible to use a dedicated software for “floating point” analyses of pixel reflection at all given wavelengths. This analysis yields spatial resolution of fluctuations in pixel luminance (i.e. the intensity of light emitted from a surface per unit area in a given direction) and chrominance (i.e. the colorimetric difference between a given color in a picture and a standard color of equal luminance), corresponding to a pixel-related spectral signature<sup>12,14-16</sup>.

There is growing evidence that mechanical vibration deeply affects stem cell dynamics and organ function<sup>17-20</sup>. Pressure waves such as those of sound could affect certain cells or their structures determining microvibrations, or even causing resonances. Evidence is still lacking that the sound generated by music instruments or the human voice during artistic live performances may differentially affect vibrational patterning in human stem cells. To address this issue, on November 7<sup>th</sup>-9<sup>th</sup>, 2016 we have organized a world premiere live experiment entitled “Cell Melodies”, held at the Centre for Music Research-San Leonardo Theatre in Bologna, Italy. On the stage, along with Milford Graves, a famous Jazz drummer based in New York, and Alessandro Bergonzoni, a renowned Italian Theatre Actor, there were live cultured human adipose-derived stem cells (hASCs), visualized with an inverted microscope equipped with a MSI system. MSI profiles were live recorded throughout each artistic performance from sep-

arate batches of stem cells. In the current study, we report and discuss the results from the Cell Melodies experiment.

## MATERIALS AND METHODS

### STEM CELL ISOLATION AND EXPOSURE CONDITIONS

According to the policies approved by the Institutional Review Boards for Human Studies local ethical committees, all tissue samples were obtained after informed consent. Human subcutaneous adipose tissue samples were obtained from li-poaspiration/liposuction procedures, using the Lipogems device, according to a recently described non-enzymatic procedure<sup>21,22</sup>.

To obtain Lipogems-derived hASCs, a volume of 1.5 ml of Lipogems product, containing approximately  $6 \times 10^4$  hASCs, was seeded in a T75 flask previously coated with human fibronectin ( $0.55 \mu\text{g}/\text{cm}^2$ ) (Sigma-Aldrich, St. Louis, MO, USA) and human collagen I-III ( $0.50 \mu\text{g}/\text{cm}^2$ ) (ABCell-Bio), cultured in Minimum Essential Medium Eagle – Alpha Modification ( $\alpha$ -MEM) supplemented with 20% heat-inactivated Fetal Bovine Serum (FBS), antibiotics (200 units/ml penicillin, 100  $\mu\text{g}/\text{ml}$  streptomycin), L-Glutamine (1%), and incubated at  $37^\circ\text{C}$  in a humidified atmosphere with 5%  $\text{CO}_2$ . The Lipogems product was maintained in culture for 10 days, with culture medium changes every 4 days, and it was subsequently eliminated completely from the supernatant. Adherent fibroblast-like cells proliferated and reached confluence after 2 weeks. These cells were subsequently detached by treatment with trypsin-EDTA (Sigma-Aldrich), and subcultured. Experiments were performed at passage 3. Two samples from a single batch of Lipogems-derived hASCs were used for the two 45 min performances of each Artist (Jazz drum solo, or Actor's dialog). Cell viability was assessed by the 3-(4, 5-dimethylthiazol-2-yl)2, 5-diphenyl-tetrazolium bromide (MTT, Sigma-Aldrich Co., St. Louis, MO, USA) assay. Time interval from the  $\text{CO}_2$  incubator in the Laboratory to the Theatre was less than 10 min. During this period, throughout each performance (max 45 min) the cap of the T75 flask was kept closed. The temperature was recorded 6 times (every 10 minutes) within the transfer container and in the theater until completion of the performance. The cells were maintained on the stage of a MSI-equipped inverted microscope for the duration of the performance (see below).

### MSI RECORDING

MSI monitoring was performed on hASCs placed on the stage of an inverted microscope (Nikon Eclipse TS 100). The microscope was positioned, at a distance of 2 meters from the Artist's site of performance, onto the wooden floor of the theater, using a concrete block between the floor and the microscopy body as a vibration isolation material. A Touptek U3CCD, an ExView HAD CCD series camera (SONY), was interfaced with the microscope optical system. It adopts Sony ExView HAD CCD sensor as the image-picking device, which is designed to drastically improve light efficiency by including near-infrared light region as a basic structure of HAD (Hole-Accumulation-Diode) sensor. The camera embeds a filter with very narrow spectral bands (10 nm): a band in the blue, two in the green, one in the red and one wideband (100 nm) in the NIR, with 1:1000,000 out-of-band cut-off.

The reason for these narrow bands is that a small change in energy is better observed in a narrow than in a wide band. The four chromatic components that work together with an IR wideband component are very sensitive to changes in luminance and chrominance, as compared with the normal response from back-illuminated color sensors. To this end, the purpose of the study was to observe slight variations in chrominance and luminance due to micro-vibrational 3D phenomena that modify the angle of incidence and refraction of the light hitting the cell structure.

A custom video analysis software was developed to process the incoming frames showing the spectral variations in amplitude and frequency, interpolating variation in the measured data within a vibrational range between 0.01 Hz and 10 Hz, providing a pseudo-coloring of the phenomenon with the aforesaid frequency values. A software algorithm allowed to calculate and subtract pixel random variation due to background noise during image acquisition, therefore allowing accurate assessment of differential changes in luminance and chrominance due to the examined vibrational pattern.

A 2-min silence, from both the Artists and the Audience, preceded each performance and was used as a control background sound in each MSI recording.

Electro-acoustic analysis of sound pressure in close vicinity (50 cm) of the optical system of the microscope was performed by the aid of a Praat software (<http://www.fon.hum.uva.nl/praat/>).



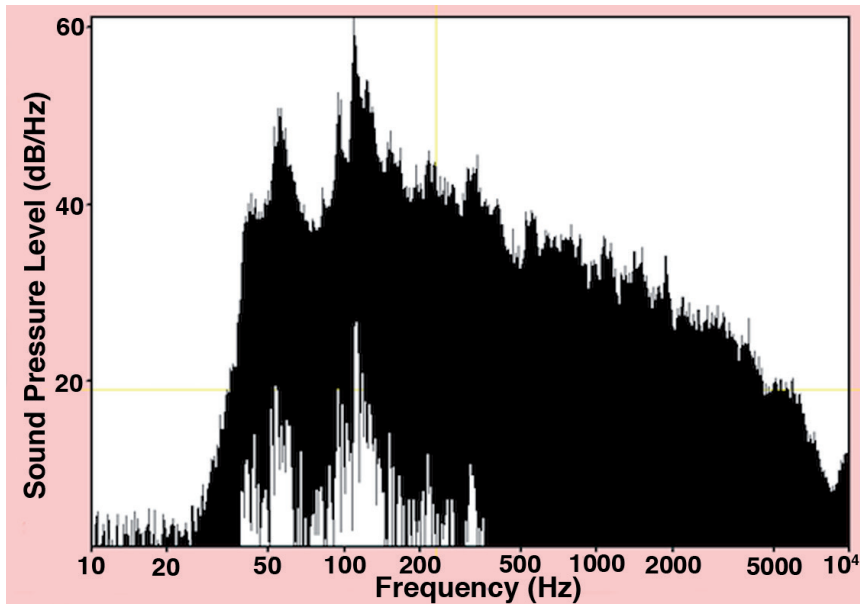


**Figure 1.** Sound exposure of hASCs during the percussion performance. The figure shows the average changes (mean  $\pm$  SD of 6 separate determinations) in sound pressure level and frequency spectrum at which hASCs were exposed during a 10 min of constant sound intensity within a 45 min performance from the Jazz drummer. Electro-acoustic analysis of sound pressure in close vicinity (50 cm) of the optical system of the microscope was performed by the aid of a Praat software (<http://www.fon.hum.uva.nl/praat/>).

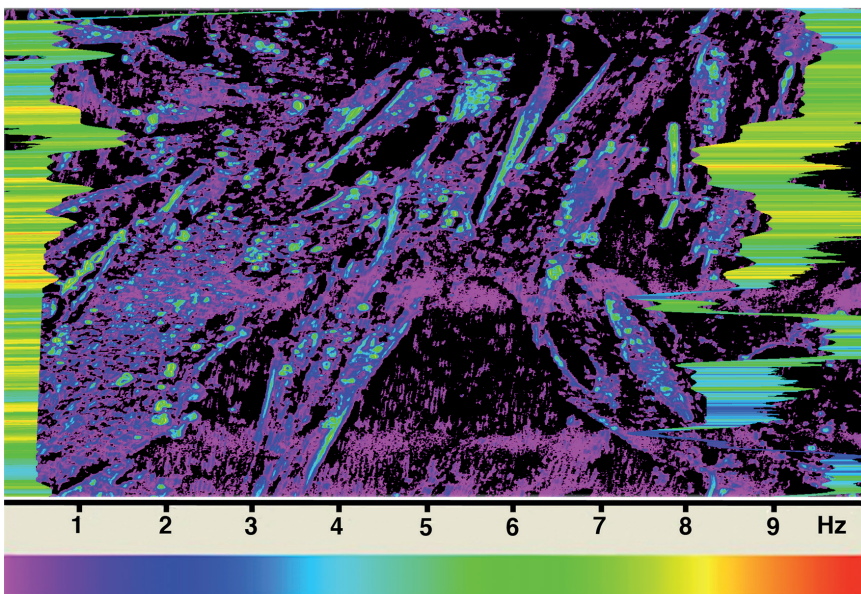
## RESULTS

The average temperature within the transfer container and in the theatre was found to be  $25 \pm 1^\circ\text{C}$ . The permanence of the cultured cells outside the  $37^\circ\text{C}$  5%  $\text{CO}_2$  incubator during the transfer and performance did not appreciably affect cell viability, as assessed in separate experiments by the 3-(4,5-dimethylthiazol-2-yl)2, 5-diphenyl-tetrazolium bromide assay.

Figure 1 depicts the average changes in the sound frequency spectrum and sound pressure level reaching the stem cell culture during a 10 min of constant sound intensity within a 45 min performance from

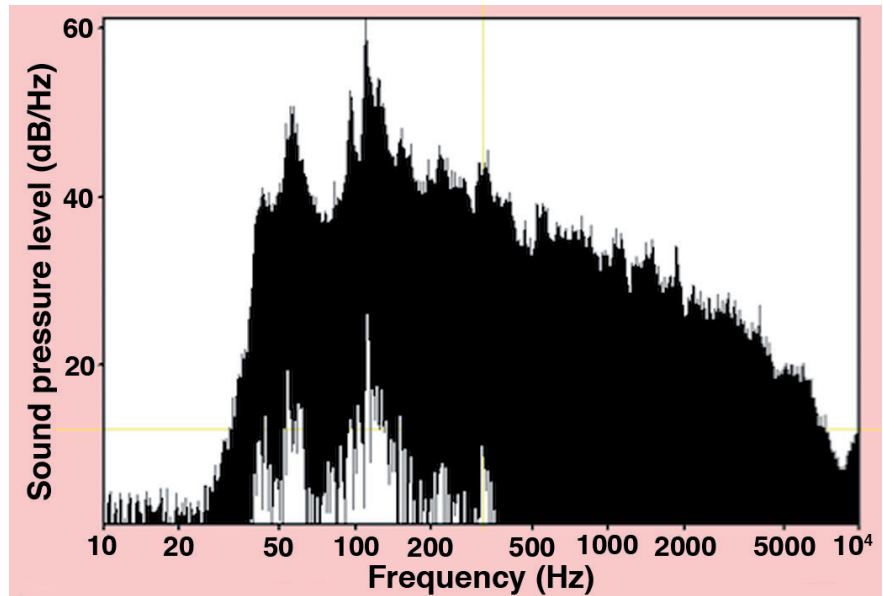
the Jazz drummer. The fundamental frequency was at about 70 Hz, producing a sound pressure level of about 50 dB. The second harmonic was at about 140 Hz, with about 60 dB in sound pressure level, being reinforced by the environmental resonance. A sequence of intermediate frequencies ranging between 10 Hz and 10 KHz was also detected, generating a 10 to 40 dB sound pressure.

Figure 2 shows the multispectral imaging of vibrational patterning exhibited by hADSCs in response to the sound path produced by the Jazz Artist, as depicted in Figure 1. The color pattern represents pseudo-colors corresponding to a vi-



**Figure 2.** MSI of hADSCs during the percussion performance. MSI analysis was performed in hADSCs exposed to the sound characteristics induced by the Jazz Drummer performance, as shown in Figure 1. Pseudocolors correspond to the vibrational scale (Hz) reported at the bottom of the figure. Fourier transform from real-time sampling of the averaged cellular vibrational frequencies emitted in response to percussion sound are shown on the left and right sides of the figure. For further details, see the description in the Results section. These data are the mean  $\pm$  SD of 6 separate determinations during the same sound recording shown in Figure 1.

**Figure 3.** Sound characteristics generated during the percussion performance reached stable features. The sound analysis was performed as described in Figure 1 in a different moment of the Jazz Drummer performance (mean  $\pm$  SD of 6 separate determinations). Note the remarkable similarity of the sound pressure and frequency spectra.



brational scale ranging between 0 and 10 Hz, as shown at the bottom of the figure. The absence of detectable vibrations is shown as a black background. In the middle of the image hADSCs appear as colored elongated shapes with color pattern often gathering cellular contours. On the left and right side of the image are the Fourier transform highlighting a real-time sampling of the averaged vibrational frequencies emitted by the sound-exposed hASCs. The colored cellular field in between is a 5-second averaged acquisition of pixelated (640 x 480, corresponding to 307,200 points) representation of cellular vibration.

Interestingly, the sound frequency spectrum and pressure level pattern sampled in a different time window of the Jazz performance showed superimposable results to those reported in Figure 1 (Figure 3). Consonant with this observation, the multispectral imaging of the vibrational patterning exhibited by hADSCs in response to the sound path was highly consistent with that shown in Figure 2 (Figure 4).

This finding indicates that the vibrational behavior of hASCs in response to the acoustic environment generated by the live performance of the Jazz musician was highly reproducible in the presence of similar acoustic (frequency and sound power) profiles.

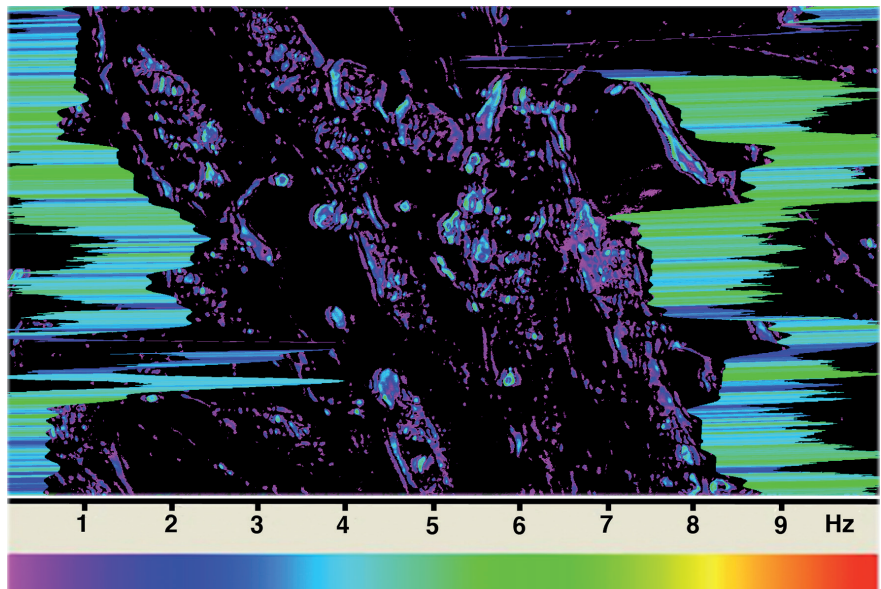


**Figure 4.** Comparable sound features are mirrored by similar MSI spectra. Stabilization of sound features as shown in Figures 1 and 3, results in similar MSI patterning as those reported in Figure 2 (see this figure for technical details). These data are the mean  $\pm$  SD of 6 separate determinations during the same sound recording shown in Figure 3.

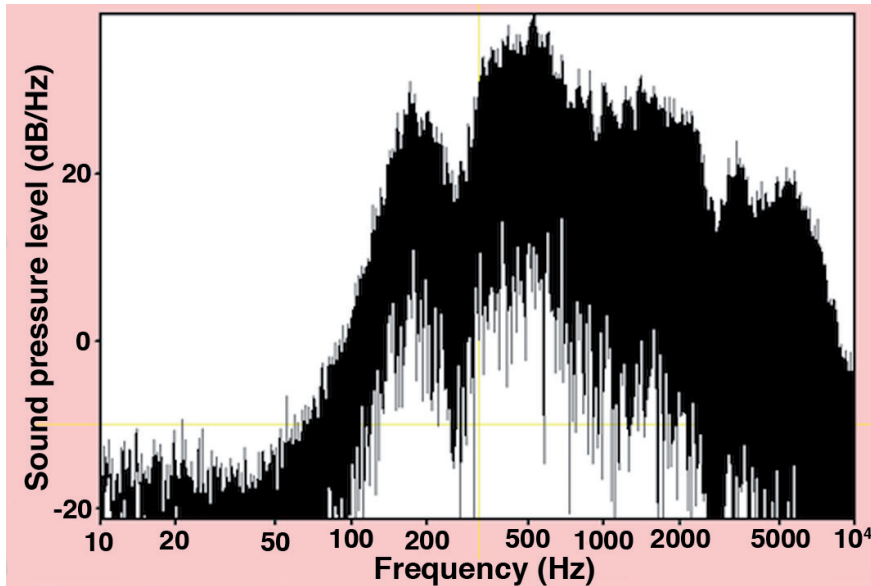


**Figure 5.** Sound exposure of hASCs during a recital with a clang voice. The Actor was placed at a distance of 2 m from the cellular field. The figure shows average changes (mean  $\pm$  SD of 6 separate determinations) in sound pressure level and frequency spectrum at which hASCs were exposed during a 10 min of constant sound intensity within a 30 min of the Actor's performance. Electro-acoustic analysis of sound pressure in close vicinity (50 cm) of the optical system of the microscope was performed by the aid of a Praat software (<http://www.fon.hum.uva.nl/praat/>).

In another set of performance in our live experiment, we aimed at investigating the vibrational response of hASCs during the exposure to the sound emitted by the human voice. In particular, we asked a theater Actor to perform with a clang voice sound at a distance of 2 m from the cellular field, or to express his recital with a whispered voice (like a prayer) at a closer distance (1 m). We made our comparative MSI analyses by choosing acoustic streams of comparable sound power but entailing different frequency patterns. Representative images of the sound power from the performance execut-

ed with a clang or whispered tone of voice are shown in Figure 5 and Figure 7, respectively. It is evident that, despite superimposable sound power levels, the frequency spectrum differed significantly among the two performances. In fact, during a 10 min of constant sound intensity within a 30 min performance, the F0 was detected at about 200 Hz during the clang voice recital (Figure 5), while it was found at about 100 Hz in the whispered voice recital (Figure 7). Moreover, an increase in harmonic intensity (Figure 7) was found in the whispered voice recording, as compared to the clang voice.

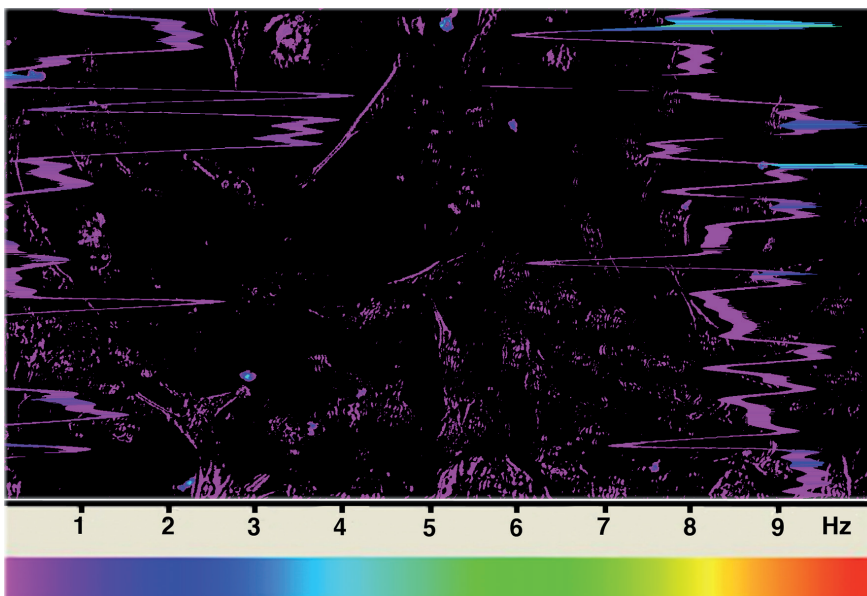
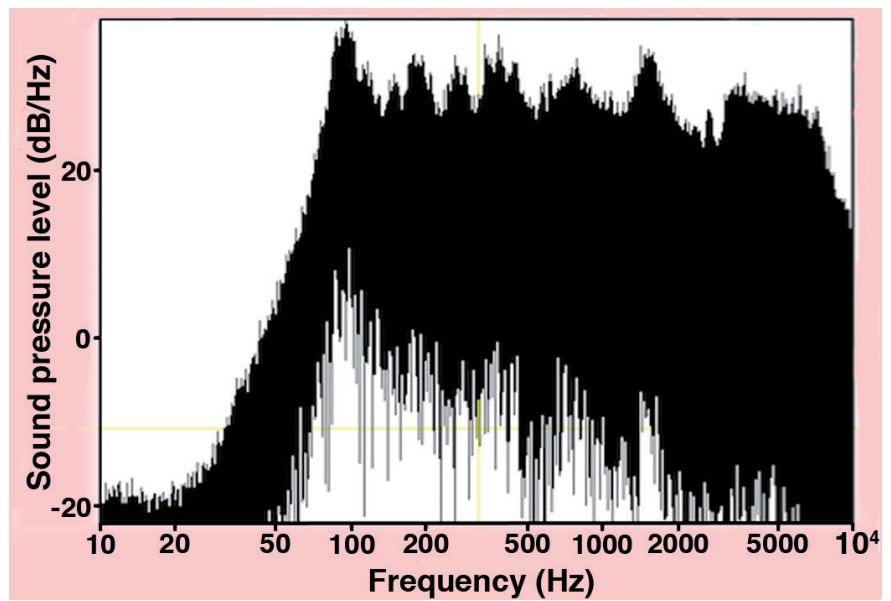


**Figure 6.** MSI of hADSCs during a recital with a clang voice. MSI analysis was performed in hADSCs exposed to the sound characteristics produced by the Actors voice, as shown in Figure 5. Pseudocolors correspond to the vibrational scale (Hz) reported at the bottom of the figure. Fourier transform from real-time sampling of the averaged cellular vibrational frequencies emitted in response to a clang sound of voice are shown on the left and right sides of the figure. For further details, see the description in the Results section. These data are the mean  $\pm$  SD of 6 separate determinations during the same sound recording shown in Figure 5.



**Figure 7.** Sound exposure of hASCs during a recital with a whispered voice. The Actor was placed at a distance of 1 m from the cellular field. The figure shows average changes (mean  $\pm$  SD of 6 separate determinations) in sound pressure level and frequency spectrum at which hASCs were exposed during a 10 min of constant sound intensity within a 30 min of the Actor's performance. This figure reports acoustic streams of comparable sound power to, but different frequency patterns from, those shown in Figure 5. Electro-acoustic analysis of sound pressure in close vicinity (50 cm) of the optical system of the microscope was performed by the aid of a Praat software (<http://www.fon.hum.uva.nl/praat/>).

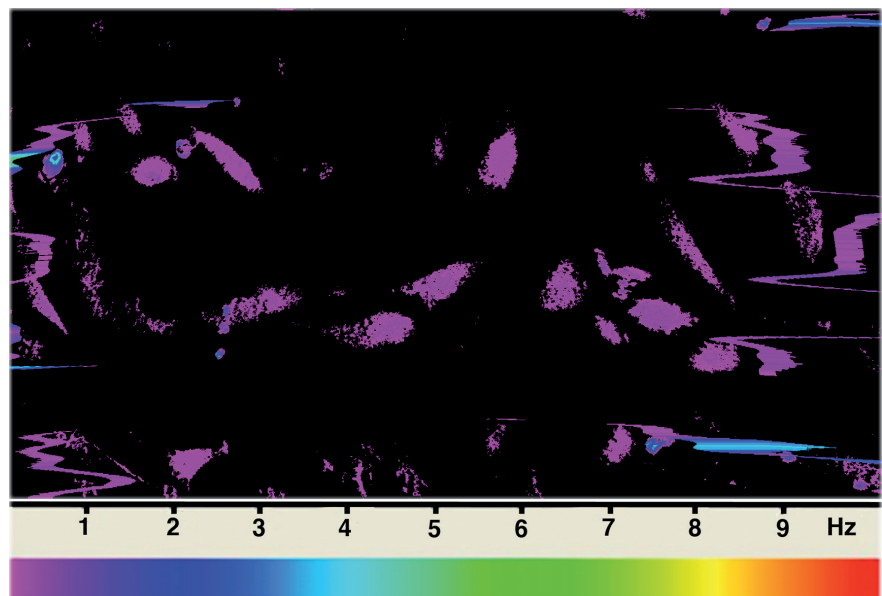


Intriguingly, the MSI profiles corresponding to the different frequency patterns exhibited remarkably different signatures, as shown in Figure 6 and Figure 8. In fact, the MSI profile corresponding to the clang sound was mainly restricted to the peripheral part of the cell in about a 50% of the hASC population (Figure 6) with no signal emerging above the background in the rest of the examined cells. On the contrary, the MSI signal was turned on within an area restricted to the nucleus of the cell in the vast majority (approximately 80%) of the hASCs that had been exposed to the whispered sound of voice (Figure 8).

## DISCUSSION

The present observations show that hASCs respond in a highly sensitive fashion to the sound emitted during music or recital live performance. MSI indicates a close relationship between the recorded spectrum of changes in chrominance and luminance resulting from the vibrational patterning of the stem cells and the sound pressure levels and their related harmonics produced by the Artists. The different sound power profiles elicited by the percussion and by the human voice were mirrored at the level of the vibrational spectrum emitted by hASCs. The MSI spectra differed in

**Figure 8.** MSI of hADSCs during a recital with whispered voice. MSI analysis was performed in hADSCs exposed to the sound characteristics produced by the Actors voice, as shown in Figure 7. Pseudocolors correspond to the vibrational scale (Hz) reported at the bottom of the figure. Fourier transform from real-time sampling of the averaged cellular vibrational frequencies emitted in response to a whispered sound of voice are shown on the left and right sides of the figure. For further details, see the description in the Results section. These data are the mean  $\pm$  SD of 6 separate determinations during the same sound recording shown in Figure 7.



the response of percussion or human voice sounds. MSI analyses showed that hASCs produced different vibrational spectra depending upon a clang or whispered voice sound. This finding indicates that, despite the fact that the MSI recordings were performed at superimposable sound power levels (see the Results section), human stem cells responded to the different frequency patterns of the Actor's voice with different spectral emissions.

The possible biological implications of the present results remain to be established. However, it is well established that a wide variety of biological processes are influenced by the nanomechanical properties of subcellular structures. An example of this is that the vibrational modes generated by the cytoskeleton and nucleoskeleton, whose resonance patterning imparts features characteristic of connectedness, can be transmitted up to and recorded from the cell surface<sup>23-25</sup>. These issues have been documented by the aid of atomic force microscopy (AFM), a tool to acquire information on the nanomechanical properties of cells<sup>6,7</sup>. With an accurate process of amplification, the frequency range of nanomechanical motions recorded by AFM can be turned into audible sounds, providing a method to study the cellular dynamics. The term introduced to identify this novel area of investigation is "Sonocytology". To this end, we have shown for the first time that cells express "vibrational" (nanomechanical) signatures of their health and multilineage repertoire<sup>7</sup>. We proposed and patented methods to use such signatures to stimulate lineage-specific commitments in undifferentiated cells.

In this regard, MSI may offer several advantages over AFM for the recording of the vibrational pattern of cells, as MSI is not affected by the bias introduced by the contact modes of the AFM cantilever tip with the cell surface, which may itself suppress weaker nanomotions, erasing relevant vibrational information.

A deeper understanding of the outcome of physical signaling from and to the cells may have relevant biomedical implication, as inferred from our recent findings showing that properly conveyed radioelectric fields are able to: (i) modulate the gene transcription of essential growth regulatory peptides in adult myocardial cells<sup>26</sup>, (ii) enhance the differentiating potential of mouse embryonic stem cells<sup>27,28</sup>, (iii) induce pluripotency in human adult stem cells, promoting their differentiation in-

to cardiac, neural, skeletal muscle and endothelial cells<sup>29</sup>, (iiii) afford direct reprogramming towards the same lineages in human somatic cells (dermal fibroblasts)<sup>30</sup>, (iiiii) reverse human stem cell aging *in vitro*<sup>31</sup>, (iiiiiii) reprogram PC12 cancer cells into dopaminergic neurons<sup>32</sup>, and (iiiii) optimize stem cell polarity<sup>33</sup>.

## CONCLUSIONS

Whether the vibrational patterning emitted by human stem cells in response to sound may have biological implications in stem cell homeostasis remains to be established. The possibility that the current observation may be relevant for human well being also remain speculative. Addressing these issues is the subject of our ongoing investigations.

## ACKNOWLEDGMENTS:

This research was supported by: Alberto Possati, Bologna, Italy. GUNA, Terapie d'Avanguardia, Milan, Italy.

## CONFLICT OF INTERESTS:

The Authors declare no conflict of interest.

## REFERENCES

1. Albrecht-Buehler G. Rudimentary form of cellular "vision". Proc Natl Acad Sci USA 1992; 89: 8288-8292.
2. Albrecht-Buehler G. A long-range attraction between aggregating 3T3 cells mediated by near-infrared light scattering. Proc Natl Acad Sci USA 2005; 102: 5050-5055.
3. Sahu S, Ghosh S, Fujita D, Bandyopadhyay A. Live visualizations of single isolated tubulin protein self-assembly via tunneling current: effect of electromagnetic pumping during spontaneous growth of microtubule. Sci Rep 2014; 4: 7303. doi: 10.1038/srep07303.
4. Havelka D, Cifra M, Kučera O, Pokorný J, Vrba J. High-frequency electric field and radiation characteristics of cellular microtubule network. J Theor Biol 2011; 286: 31-40.
5. Sahu S, Ghosh S, Hirata K, Fujita D, Bandyopadhyay A. Multi-level memory-switching properties of a single brain microtubule. Appl Phys Lett 2013; 102: 123701. doi: 10.1063/1.4793995.
6. Pelling AE, Sehati S, Gralla EB, Valentine JS, Gimzewski JK. Local nanomechanical motion of the cell wall of *Saccharomyces cerevisiae*. Science 2004; 305: 1147-1150.
7. Gimzewski JK, Pelling A, Ventura C. INTERNATIONAL PATENT: International Publication Number WO 2008/105919 A2, International Publication Date 4 September 2008. Title: Nanomechanical Characterization of Cellular Activity.



8. Uzer G, Thompson WR, Sen B, Xie Z, Yen SS, Miller S, Bas G, Styner M, Rubin CT, Judex S, Burr ridge K, Rubin J. Cell Mechanosensitivity to Extremely Low-Magnitude Signals Is Enabled by a LINCed Nucleus. *Stem Cells* 2015; 33: 2063-2076.
9. Schaap IA, Carrasco C, de Pablo PJ, Schmidt CF. Kinesin walks the line: single motors observed by atomic force microscopy. *Biophys J* 2011; 100: 2450-2456.
10. Cosic I, Cosic D, Lazar K. Is it possible to predict electromagnetic resonances in proteins, DNA and RNA? *EPJ Nonlinear Biomedical Physics* 2015; 3: 5 doi: 10.1140/s40366-015-0020-6.
11. Acbas G, Niessen KA, Snell EH, Markelz AG. Optical measurements of long-range protein vibrations. *Nat Commun* 2014; 5: 3076. doi: 10.1038/ncomms4076.
12. Gao L, Smith RT. Optical hyperspectral imaging in microscopy and spectroscopy - a review of data acquisition. *J Biophotonics* 2015; 8: 441-456.
13. Lu G, Halig L, Wang D, Qin X, Chen ZG, Fei B. Spectral-spatial classification for noninvasive cancer detection using hyperspectral imaging. *J Biomed Opt* 2014; 19: 106004. doi: 10.1117/1.JBO.19.10.106004.
14. Cheng JX, Xie XS. Vibrational spectroscopic imaging of living systems: An emerging platform for biology and medicine. *Science* 2015; 350: aaa8870. doi: 10.1126/science.aaa8870.
15. Gosnell ME, Anwer AG, Mahbub SB, Menon Perinchery S, Inglis DW, Adhikary PP, Jazayeri JA, Cahill MA, Saad S, Pollock CA, Sutton-McDowall ML, Thompson JG, Goldys EM. Quantitative non-invasive cell characterisation and discrimination based on multispectral autofluorescence features. *Sci Rep* 2016; 6: 23453. doi: 10.1038/srep23453.
16. Gosnell ME, Anwer AG, Cassano JC, Sue CM, Goldys EM. Functional hyperspectral imaging captures subtle details of cell metabolism in olfactory neurosphere cells, disease-specific models of neurodegenerative disorders. *Biochim Biophys Acta* 2016; 1863: 56-63.
17. Rubin C, Turner AS, Bain S, Mallinckrodt C, McLeod K. Anabolism. Low mechanical signals strengthen long bones. *Nature* 2001; 412: 603-604.
18. Rubin CT, Capilla E, Luu YK, Busa B, Crawford H, Nolan DJ, Mittal V, Rosen CJ, Pessin JE, Judex S. Adipogenesis is inhibited by brief, daily exposure to high-frequency, extremely low-magnitude mechanical signals. *Proc Natl Acad Sci U S A* 2007; 104: 17879-17884.
19. Sen B, Styner M, Xie Z, Case N, Rubin CT, Rubin J. Mechanical loading regulates NFATc1 and beta-catenin signaling through a GSK3beta control node. *J Biol Chem* 2009; 284: 34607-34617.
20. Ozcivici E, Luu YK, Adler B, Qin YX, Rubin J, Judex S, Rubin CT. Mechanical signals as anabolic agents in bone. *Nat Rev Rheumatol* 2010; 6: 50-59.
21. Bianchi F, Maioli M, Leonardi E, Olivi E, Pasquinelli G, Valente S, Mendez AJ, Ricordi C, Raffaini M, Tremolada C, Ventura C. A new nonenzymatic method and device to obtain a fat tissue derivative highly enriched in pericyte-like elements by mild mechanical forces from human lipoaspirates. *Cell Transplant* 2013; 22: 2063-2077.
22. Bianchi F, Olivi E, Baldassarre M, Giannone FA, Laggetta M, Valente S, Cavallini C, Tassinari R, Canaider S, Pasquinelli G, Tremolada C, Ventura C. Lipogems, a New Modality of Fat Tissue Handling to Enhance Tissue Repair in Chronic Hind Limb Ischemia. *CellR4* 2014; 2: e1289.
23. Uzer G, Pongkitwitoon S, Ete Chan M, Judex S. Vibration induced osteogenic commitment of mesenchymal stem cells is enhanced by cytoskeletal remodeling but not fluid shear. *J Biomech* 2013; 46: 2296-2302.
24. Uzer G, Thompson WR, Sen B, Xie Z, Yen SS, Miller S, Bas G, Styner M, Rubin CT, Judex S, Burr ridge K, Rubin J. Cell mechanosensitivity to extremely low-magnitude signals is enabled by a LINCed nucleus. *Stem Cells* 2015; 33: 2063-2076.
25. Ventura C, Tavazzi L. Biophysical signalling from and to the (stem) cells: a novel path to regenerative medicine. *Eur J Heart Fail* 2016; 18: 1405-1407.
26. Ventura C, Maioli M, Pintus G, Gottardi G, Bersani F. Elf-pulsed magnetic fields modulate opioid peptide gene expression in myocardial cells. *Cardiovasc Res* 2000; 45: 1054-1064.
27. Ventura C, Maioli M, Asara Y, Santoni D, Mesirca P, Remondini D, Bersani F. Turning on stem cell cardiogenesis with extremely low frequency magnetic fields. *FASEB J* 2005; 19: 155-157.
28. Maioli M, Rinaldi S, Santaniello S, Castagna A, Pigliaru G, Gualini S, Fontani V, Ventura C. Radio frequency energy loop primes cardiac, neuronal, and skeletal muscle differentiation in mouse embryonic stem cells: a new tool for improving tissue regeneration. *Cell Transplant* 2012; 21: 1225-1233.
29. Maioli M, Rinaldi S, Santaniello S, Castagna A, Pigliaru G, Delitala A, Bianchi F, Tremolada C, Fontani V, Ventura C. Radio electric asymmetric conveyed fields and human adipose-derived stem cells obtained with a non-enzymatic method and device: a novel approach to multipotency. *Cell Transplant* 2014; 23: 1489-1500.
30. Maioli M, Rinaldi S, Santaniello S, Castagna A, Pigliaru G, Gualini S, Cavallini C, Fontani V, Ventura C. Radio electric conveyed fields directly reprogram human dermal-skin fibroblasts toward cardiac-, neuronal-, and skeletal muscle-like lineages. *Cell Transplant* 2013; 22: 1227-1235.
31. Rinaldi S, Maioli M, Pigliaru G, Castagna A, Santaniello S, Basoli V, Fontani V, Ventura C. Stem cell senescence. Effects of REAC technology on telomerase-independent and telomerase-dependent pathways. *Sci Rep* 2014; 4: 6373. doi: 10.1038/srep06373.
32. Maioli M, Rinaldi S, Migheli R, Pigliaru G, Rocchitta G, Santaniello S, Basoli V, Castagna A, Fontani V, Ventura C, Serra PA. Neurological morphofunctional differentiation induced by REAC technology in PC12. A neuro protective model for Parkinson's disease. *Sci Rep* 2015; 5: 10439. doi: 10.1038/srep10439.
33. Maioli M, Rinaldi S, Pigliaru G, Santaniello S, Basoli V, Castagna A, Fontani V, Ventura C. REAC technology and hyaluron synthase 2, an interesting network to slow down stem cell senescence. *Sci Rep* 2016; 6: 28682. doi: 10.1038/srep28682.